

High Optical Quality Polycrystalline Indium Phosphide Grown on Metal Substrates by MOCVD for Photovoltaic Applications

Maxwell Zheng



Electrical Engineering and Computer Sciences
University of California at Berkeley

Technical Report No. UCB/EECS-2012-39

<http://www.eecs.berkeley.edu/Pubs/TechRpts/2012/EECS-2012-39.html>

April 4, 2012

Copyright © 2012, by the author(s).
All rights reserved.

Permission to make digital or hard copies of all or part of this work for personal or classroom use is granted without fee provided that copies are not made or distributed for profit or commercial advantage and that copies bear this notice and the full citation on the first page. To copy otherwise, to republish, to post on servers or to redistribute to lists, requires prior specific permission.

**High Optical Quality Polycrystalline Indium Phosphide Grown on Metal
Substrates by MOCVD for Photovoltaic Applications**

by Maxwell S. Zheng

Research Project

Submitted to the Department of Electrical Engineering and Computer Sciences, University of California at Berkeley, in partial satisfaction of the requirements for the degree of **Master of Science, Plan II**.

Approval for the Report and Comprehensive Examination:

Committee:

Professor Ali Javey
Research Advisor

(Date)

* * * * *

Professor Ming Wu
Second Reader

(Date)

Table of Contents:

Chapter 1: Introduction	3
Chapter 2: High Optical Quality Polycrystalline Indium Phosphide Grown on Metal Substrates by MOCVD for Photovoltaic Applications	5
Motivations and Prior Art.....	5
Fabrication.....	7
Characterization.....	9
Summary and Outlook.....	16
References.....	17

List of Figures and Tables:

Figure 1: Fabrication scheme and large scale appearance.....	8
Figure 2: SEM top view and cross section, and TEM of grain boundaries and InP/Mo interface.....	9
Figure 3: SEM and TEM of stacking faults formed at low growth temperatures.....	10
Figure 4: X-ray diffraction dependence on growth temperature.....	11
Figure 5: Raman peak dependence on growth temperature.....	12
Figure 6: Photoluminescence dependence on growth temperature.....	13
Table 1: Photoluminescence peak positions and full-width-at-half-maximum dependence on growth temperature.....	14

Chapter 1

My broad research interests are in grid-level green energy generation and storage. Both of these are necessary for humanity's future. The need for green/renewable/sustainable energy is obvious, from either the peak oil or global warming arguments. But as the dominant technologies (wind, solar) are still vulnerable to the whims of nature, grid-level energy storage (MWh, GWh) is needed to change these from interruptibles to dispatchables and truly scale. These two, generation and storage, are inextricably linked going forward.

My current research falls under the area of energy generation, and specifically III-V photovoltaics. Here, the goal is high-efficiency, low-cost terrestrial solar cells for electricity generation. As a commodity industry, cost is the most critical issue, and the metric used is dollars per watt. However, most fabrication, installation, and maintenance costs scale directly with area. In addition, for most projects, the area is fixed and so an equally important metric to consider is dollars per square meter. Hence, the true goal is to maximize power output for a given areal footprint, which is dictated by the power conversion efficiency. This is the reason there is a relentless focus on high-efficiency, and future solar cells will need to reach the 40-70% efficiency range to truly become ubiquitous.

III-Vs are a natural choice to achieve this goal. They have the highest demonstrated efficiencies for single-junction solar cells. They span a large range of band gaps, and can be combined in multi-junction cells to cover nearly the entire solar spectrum. The large absorption coefficients also dictate minimal use of material. However, the complex and costly processing schemes have been a large enough disadvantage to limit them mainly to space applications.

My goal is to explore low-cost manufacturing processes for producing III-V solar cells, both single- and multi-junction. Along these lines, this project, "High Optical Quality

Polycrystalline Indium Phosphide Grown on Metal Substrates by MOCVD” is an effort to relax the traditional single-crystal requirement and see if III-Vs are amenable to high-throughput, roll-to-roll processes. The ability to use flexible metal substrates is key in this goal, and this project is the first step in producing low-cost multi-junction terrestrial III-V solar cells.

The following chapter presents a preliminary work in this area. The intrinsic advantages of III-V semiconductors for solar cells have been hobbled by the lack of low-cost substrates and processes, which has thus far limited market success of III-V solar cells. Here we are exploring a non-traditional approach which addresses these drawbacks. High optical quality polycrystalline InP films have been grown on non-epitaxial molybdenum substrates. Remarkably, these films with micron-sized grains have similar photoluminescence qualities as single-crystalline InP, and show great promise for high-efficiency, low-cost solar cells.

Chapter 2

The following work has been submitted for publication in a near identical form under the title “High Optical Quality Polycrystalline Indium Phosphide Grown on Metal Substrates by MOCVD” with the following authors: Maxwell Zheng, Zhibin Yu, Tae Joon Seok, Yu-Ze Chen, Rehan Kapadia, Kuniharu Takei, Shaul Aloni, Joel W. Ager, Ming Wu, Yu-Lun Chueh, and Ali Javey

Motivations and Prior Art

III-V semiconductor solar cells have demonstrated the highest power conversion efficiencies to date.^[1] Specifically, InP and GaAs have the most ideal band gaps and highest theoretical efficiencies for single-junction cells. However, the cost of III-V solar cells has historically been too high to be practical outside of specialty applications. This stems from the cost of raw materials, need for a lattice-matched substrate for epitaxial growth of single crystals, and complex epitaxial growth processes.^{[2],[3]} To address these issues layer transfer techniques have been explored in the past, where thin epitaxial films of GaAs and InP are selectively peeled and transferred from the growth substrate to a user-defined receiver substrate.^{[3]-[8]} This process enables for the growth substrate to be used multiple times, thereby potentially lowering the manufacturing cost. Here, we explore a different approach where thin (~1-3 μm) layers of III-Vs are *directly* grown on metal substrates, including thin foils. This minimizes the amount of raw material used and swaps the high-cost substrate for a low-cost one. In addition, metal foils lend themselves to low-cost roll-to-roll processing schemes, act as excellent diffusion barriers to the environment, and exhibit high thermal stability.

Thin film growth on non-epitaxial substrates invariably results in polycrystalline (poly) materials which presents certain constraints and challenges. In particular, the increased surface/interface area and grain boundaries may act as efficient recombination centers for photogenerated minority carriers. Thus, the use of materials with a low surface recombination

velocity (SRV) is required to ensure high efficiency poly III-V solar cells. Untreated InP has a drastically lower SRV ($\sim 10^3 \text{ cm s}^{-1}$)^{[9],[15]} as compared to GaAs ($\sim 10^6 \text{ cm s}^{-1}$),^{[15],[16]} making it an ideal candidate for efficient poly cells. However, while poly-GaAs has been widely explored in the past,^{[17],[18]} there have been few reports of poly-InP in terms of growth techniques,^{[19]-[21]} material quality,^{[9],[22]} or device performance.^{[23],[24]}

Here we report high optical-quality poly-InP thin films grown on molybdenum substrates, both thin films and foils, by metalorganic chemical vapor deposition (MOCVD). The materials and optical characteristics of the grown films are systematically explored as a function of growth temperature. Poly-InP films grown at the optimal temperature exhibit highly promising properties that potentially enable low-cost, yet efficient III-V solar cells in the near future.

Fabrication

The choice of substrate metal is critical for obtaining high quality poly-InP films. At the growth temperature, it should have low solubility of both indium and phosphorus. Ideally, it should either not form indium alloys or metal phosphides, or if it does, the growth should be self-limiting. In addition, it should have a similar thermal expansion coefficient as InP.^[24] From metal-P and metal-In phase diagrams, Mo and W meet the above criteria the best. For Mo in particular, there are no intermetallics at the growth temperature, and the solubility of In is very low. There are few Mo-P compounds, and no solid solutions. Here, we have chosen to focus on Mo, both in the form of thin foils and thin films. The Mo foils used were 25 μm thick and cleaned with acetone and isopropanol prior to growth. In parallel, Si/SiO₂ (thermal oxide, 50 nm thickness) handling wafers with a sputtered Cr (5 nm thickness) adhesion layer and Mo (50 nm thickness) top film were explored as a growth substrate.

Subsequently, InP thin films were grown on top of these Mo substrates by MOCVD as schematically illustrated in **Figure 1a**. Optical images of InP thin films ($\sim 2 \mu\text{m}$ thickness) grown on flexible Mo foil and sputtered Mo thin film substrates (510 °C and 75 minutes) are shown in Fig. 1b and 1c, respectively. Thus far, we have grown uniform films over $\sim 40 \text{ cm}^2$ foils and 3” diameter wafers, limited only by the sample holder size of the MOCVD equipment used in this study. As evident from visual inspection, the grown InP films exhibit large area uniformity and continuity. The foils can flex quite easily (Fig. 1b) without peeling or flaking of the InP on top. In general, the growth properties were found to be similar between the two types of substrates. Thus, from here on we primarily present the growth data on the Mo thin film substrate.

The MOCVD system used was a Thomas Swann 3x2 CCS MOCVD. The chamber was a vertical cold-wall showerhead configuration. The susceptor held 3” wafers and the rotation rate was fixed at 30 RPM. The precursors were Trimethylindium (TMIn) from Akzo Nobel and Tert-

butylphosphine (TBP) from Dockweiler Chemicals. They were held at 20 °C and 10 °C, respectively. TMIIn was flowed at $\sim 1.2\text{E-}5$ mol/min and TBP at $\sim 2.4\text{E-}3$ mol/min, giving a [V]/[III] molar ratio of ~ 200 . Total flow of H_2 and precursors was 11.5 L/min. Growth temperatures ranged from 445 °C to 545 °C. Growth times explored were 5-75 minutes, with 75 minutes used for the data in this paper. The chamber pressure was fixed at 76 torr.

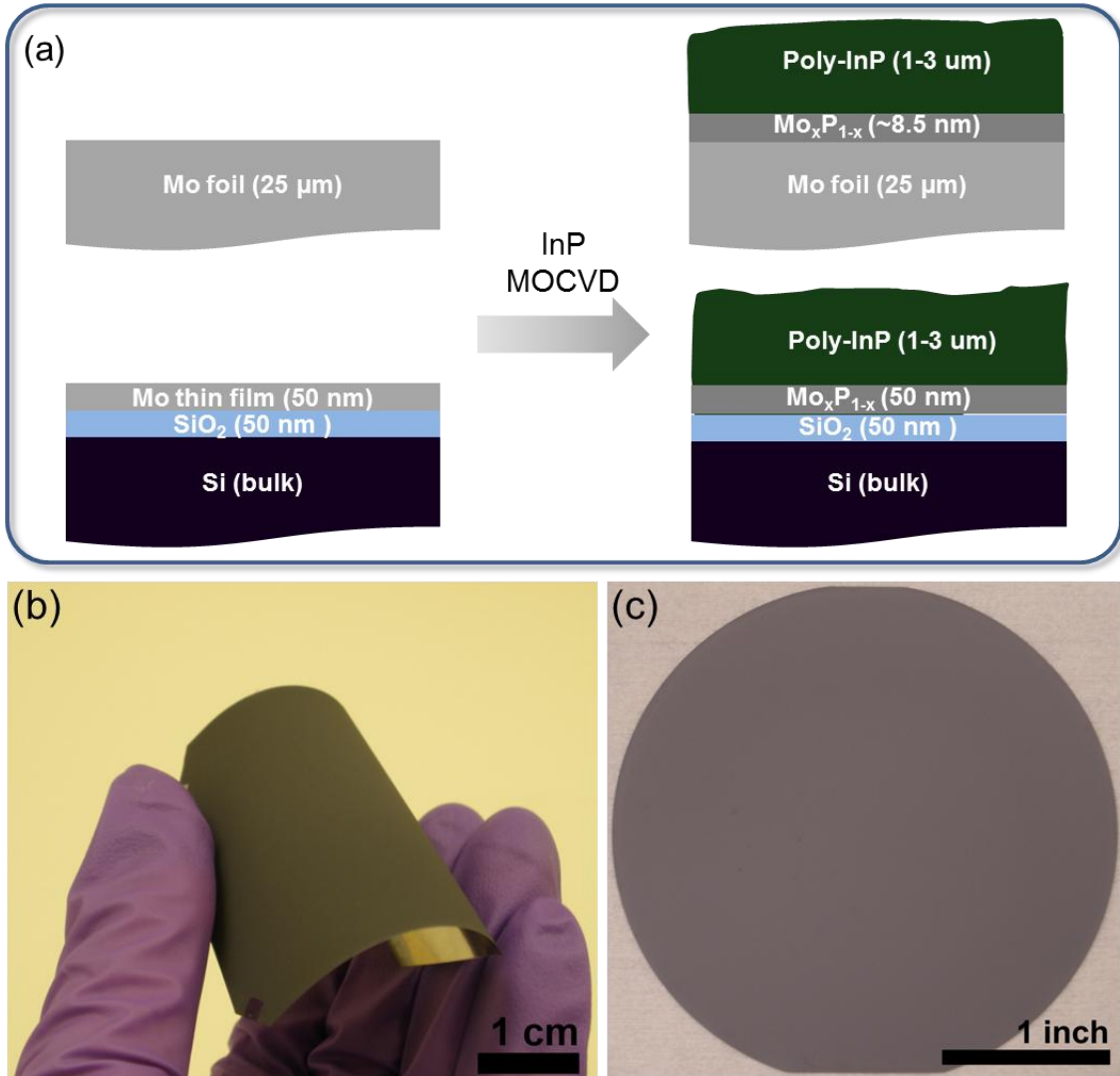


Figure 1. (a) Poly-InP fabrication scheme. (b) Poly-InP on flexible molybdenum foil. (c) Poly-InP on sputtered Mo on 3" wafer.

Characterization

In this work, we primarily focus on the effects of growth time and temperature. **Figure 2** shows top-and side-view SEM images of a representative InP thin film ($\sim 3 \mu\text{m}$ thickness) grown on a Mo thin film. The growth temperature and time were $520 \text{ }^\circ\text{C}$ and 75 min, respectively. The grown InP films are poly-crystalline and continuous (Fig. 2a,b). The grains generally extend continuously to the substrate, but are oriented randomly. The average grain size and surface roughness for this growth condition are $\sim 2 \mu\text{m}$ and 200 nm, respectively – both of which highly depend on the growth temperature.

From SEM analyses, the grain sizes range from $\sim 0.5 \mu\text{m}$ for $445 \text{ }^\circ\text{C}$ growth temperature to $\sim 10 \mu\text{m}$ for $545 \text{ }^\circ\text{C}$. While the grain size increases with temperature, the grown InP is not

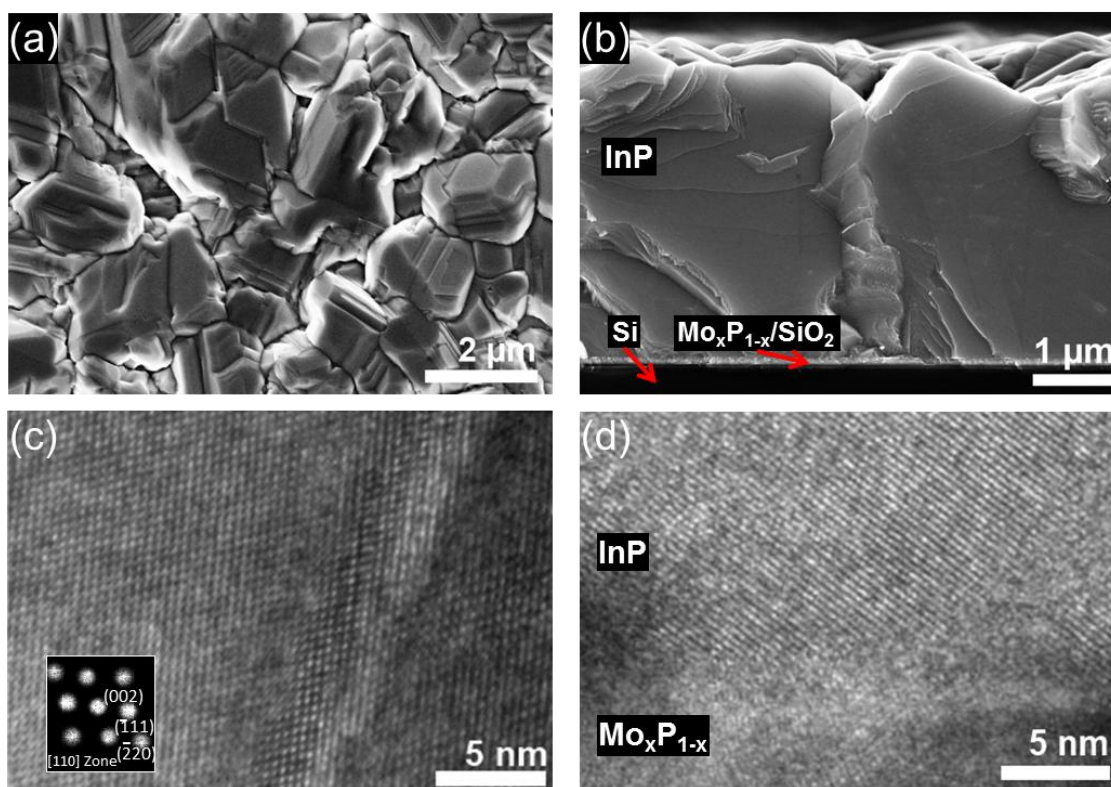


Figure 2. (a) SEM top view of poly-InP grown at $520 \text{ }^\circ\text{C}$ for 75 minutes. (b) Cross-sectional SEM image of poly-InP grown on a Mo thin film at $520 \text{ }^\circ\text{C}$ for 75 minutes. The InP is on top of $\sim 50 \text{ nm}$ $\text{Mo}_x\text{P}_{1-x}/50 \text{ nm}$ SiO_2/Si . (c) TEM image at a grain boundary. Inset shows FFT from within the left grain. (d) TEM of interface between InP and $\text{Mo}/\text{Mo}_x\text{P}_{1-x}$.

continuous at ≥ 545 °C for a fixed growth time of 75 min. This observation is expected given the reduced number of nucleation sites at higher temperatures. At growth temperatures of ≤ 500 °C, striations are clearly present within each grain oriented parallel to the substrate based on SEM inspection. Upon closer TEM examination, these indicate stacking faults (**Figure 3**). Each layer appears to consist of ~ 10 -100 close packed planes. Similar stacking faults and twinning have been observed in metalorganic vapor phase epitaxy grown InP nanowires in the [111] direction.^{[25],[26]} The data is also consistent with the known low stacking fault energy of InP.^[27] However, at growth temperatures of ≥ 520 °C, the density of stacking faults are drastically reduced with only a minimal number of such defects being evident in TEM analysis (Fig. 2c). Altogether, crystal quality appears to be higher at higher growth temperatures. These dueling constraints of crystal quality and film continuity dictate that 520 °C is the optimal growth temperature for a single growth stage of 75 minutes.

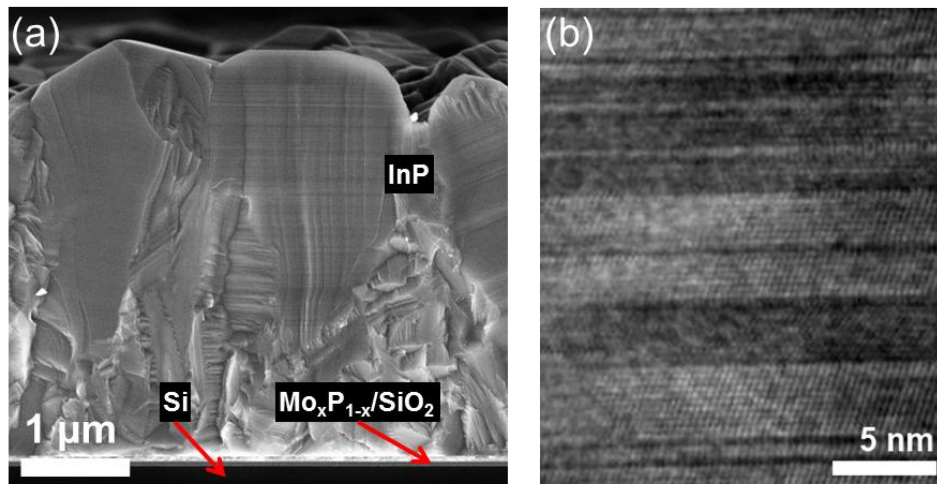


Figure 3. (a) Side view SEM image of sample grown on a Mo thin film at 500 °C for 75 minutes. A grain without striations (left) is shown next to two with horizontal striations (right). (b) TEM image of same sample showing stacking faults.

Further, TEM study indicates the interface between InP and Mo is continuous and free of voids, as seen in Figure 2d. Composition analysis reveals significant phosphorus content throughout the initial 50 nm Mo layer. It appears to be composed of a mixture of Mo and Mo_xP_{1-x}.

phases, where x ranges from ~ 0.8 to ~ 0.5 from low to high growth temperatures. In contrast, InP on Mo foil samples showed a similar $\text{Mo}_x\text{P}_{1-x}$ layer, where x ranged from ~ 0.6 to ~ 0.4 . However, this layer was self-limited to a thickness of only ~ 8.5 nm. This is attributed to the larger grain sizes of the foil vs. the sputtered Mo, and corresponding lower reactivity. Close examination reveals that in some locations, the InP lattice matches that of the underlying $\text{Mo}_x\text{P}_{1-x}$, suggesting a high quality interface. SEM images were taken on a Zeiss Gemini Ultra-55. TEM was performed using a JEOL-3000F. Note that in contrast to the results here, Ni foil substrates in the same growth conditions showed an uncontrollable reaction with phosphorus and indium. This is consistent with presence of solid solutions at the growth temperatures in the In-Ni and Ni-P phase diagrams. The surface becomes pitted and cracked and no InP film was able to grow.

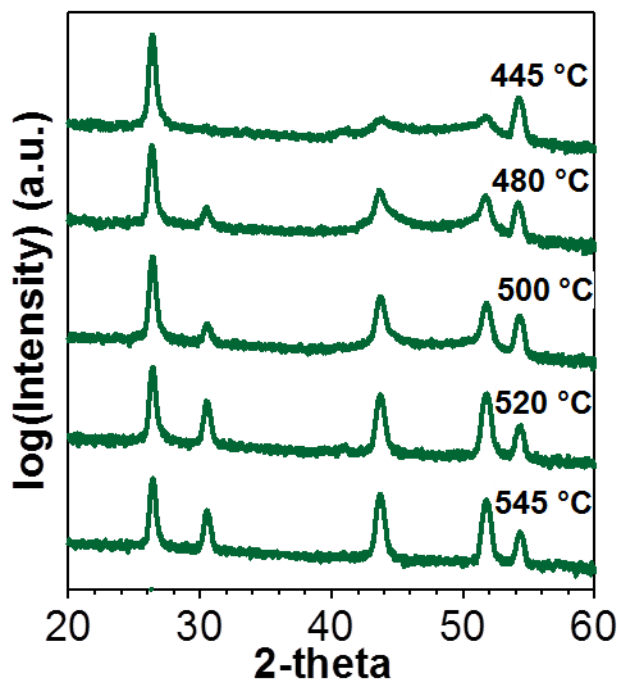


Figure 4. XRD spectra as a function of growth temperature. Curves are normalized to the (111) peak and offset. Inset, log scale, shows the gradual narrowing of the (220) and (311) peaks. Reference data are from the ICDD PDF. From left to right the first five peaks are: (111), (200), (220), (311), and (222).

The grown InP films were characterized by XRD (**Figure 4**). The XRD analysis further shows texture at lower growth temperatures, with only the (111) and (222) peaks noticeable. The

peak positions match those of zincblende InP.^{[28],[29]} As the growth temperature increases, additional peaks appear, indicating the grains become more randomly oriented. At the highest growth temperature of 545 °C, the relative peak intensities are a close match to the ICDD powder reference.^[29] In addition, the line widths of the (220) and (311) peaks get progressively narrower as growth temperature increases, indicating a greater level of crystallinity. There is no evidence of wurtzite InP peaks,^[28] especially the (0002) peak which would show up close to (111) zincblende peak, indicating that the stacking faults do not result in a phase change from zincblende to wurtzite. The XRD was taken on a Bruker AXS D8 Discover GADDS XRD Diffractometer system.

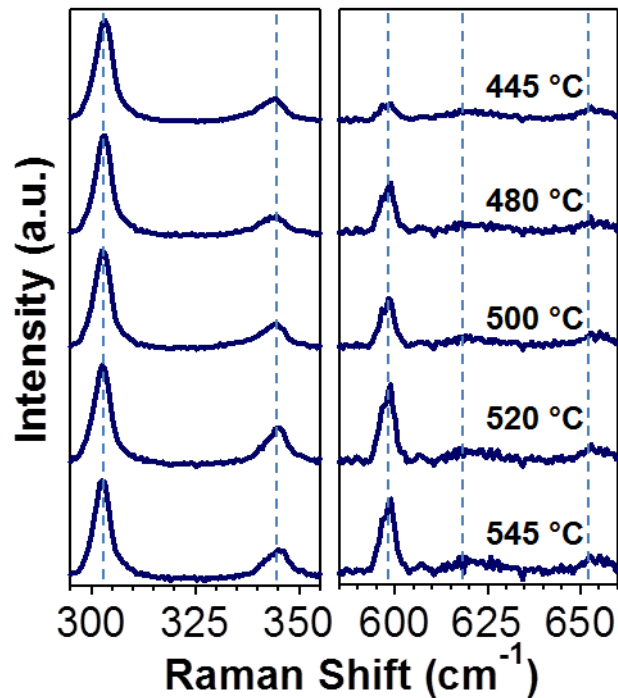


Figure 5. Room temperature Raman. Data is normalized to the Γ TO peak and offset. The left graph shows the first order peaks, Γ TO and Γ LO, from left to right. The right graph shows second order peaks, X LO + X TO, 2Γ TO, and Γ LO + Γ TO, from left to right. Intensity of data in right graph is 5x.

Raman spectra (**Figure 5**) for films grown at all temperatures (445 °C – 545 °C) match well with that reported in the literature for a single-crystalline InP substrate.^{[30]-[32]} The first order anti-Stokes Γ TO and Γ LO peaks show up at $\sim 303 \text{ cm}^{-1}$ and $\sim 344 \text{ cm}^{-1}$ respectively. The data are all

normalized to the Γ TO peak intensity. The relative intensity of the Γ LO peak increases slightly with growth temperature. In addition, the Γ LO peak shows a pronounced asymmetry towards lower energy. Second order features corresponding to the XLO + XTO, 2Γ TO, and Γ LO + Γ TO interactions also appeared.^{[30],[32]} Of these, only the XLO + XTO feature intensity showed a strong correlation with growth temperature. While the intensity increases with growth temperature, the shape remains unchanged. The features here are consistent with a randomly oriented poly-InP film. The excitation source for the backscatter Raman data was the 488 nm line from an Ar ion laser. The uncertainty of the Raman data is limited to $\pm 0.3 \text{ cm}^{-1}$.

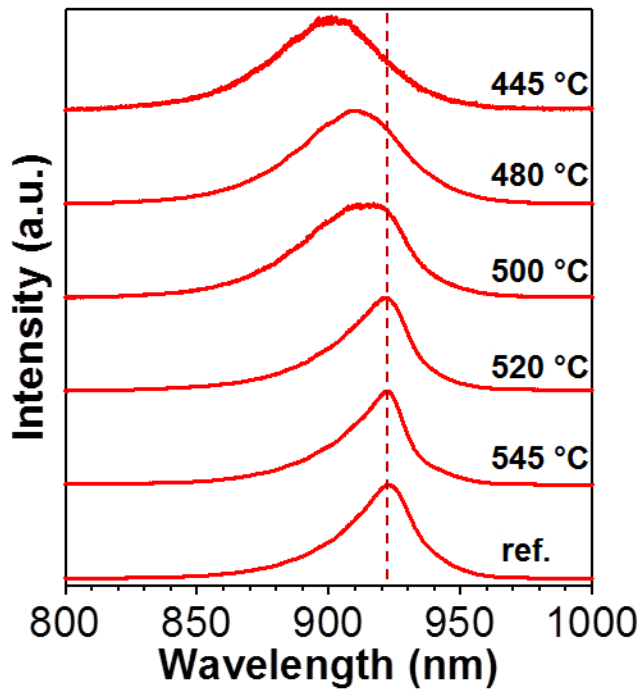


Figure 6. Room temperature PL change with growth temperature. Higher growth temperatures exhibit near identical shape and position as a single crystal reference. Curves are normalized and offset.

Room temperature micro-PL data also shows a clear trend of increasing quality with growth temperature (**Figure 6**). As a metric, we compare our poly-InP PL spectra to a single crystal InP reference. At the two highest growth temperatures (520 °C and 545 °C), the peak

position, full-width-at-half-maximum (FWHM), and shape are nearly identical to a single-crystal reference sample. This is evidence of the high optical quality of the material. At lower growth temperatures, the spectra are blue-shifted, FWHM is broad, and the shape is symmetric. The trend is summarized in **Table 1**. Note that the 520 °C and 545 °C peaks at ~922 nm correspond to the direct band gap energy of ~1.34 eV,^{[33],[34]} matching closely the expected band-gap of InP, whereas the 445 °C peak at ~898.5 nm corresponds to ~1.38 eV. Such blue-shifts have been observed for InP nanowires with stacking faults, and have been attributed to the presence of the wurtzite phase or quantum confinement, both of which increase the band gap.^{[25],[35]} While there is clearly a correlation between stacking fault prevalence due to growth temperature and PL characteristics in our InP, the SEM and XRD data don't support the same conclusions as those reached in the literature.

Growth temperature (°C)	Peak Position (nm)	FWHM (nm)
445	898.5	46
480	908.8	46
500	917.0	45
520	921.6	30
545	922.4	26
c-InP	923.4	28

Table 1. PL peak positions and FWHMs as a function of growth temperature.

Also important to note is that the PL feature from the 500 °C sample is plainly composed of two overlapping peaks, as can be seen by the asymmetry and flat top. Moreover, the relative intensities of the two contributions varied as the sample was scanned laterally (not shown). This is consistent with the SEM/TEM analyses, which shows grains with stacking faults next to those without such defects. There is also a clear transition temperature between 500 °C and 520 °C

where the optical transitions corresponding to the higher energy peak are totally suppressed, leaving only the peak corresponding to bulk zincblende InP. This possibly corresponds to the elimination of stacking faults. There is a strong correlation between the presence of stacking faults and the higher energy PL feature. However, without conclusive evidence and a satisfactory model for this hypothesis, we cannot establish a causal relationship. The possibility of other defects introduced at low growth temperatures cannot be ruled out as the source of the PL trend. Based on the PL characteristics, the optimal growth temperature is 520 °C. At this growth temperature, there are no PL features remaining that do not appear in the single crystal reference. The PL excitation source was a 785 nm laser with ~ 30 μm spot size, and the detector was a silicon CCD. Note that at this excitation, the penetration depth is ~ 290 nm, so carriers are being generated mainly in the top quarter of the films. The reference InP sample was (100) orientation n-type doped with zinc to $\sim 10^{17}$ cm^{-3} .

Summary and Outlook

To summarize, we have demonstrated high optical quality InP grown on metal substrates. The resulting films are composed of micron-sized grains, and importantly show nearly identical PL and Raman spectral shape and position as those of a single-crystal reference. In the future, further characterization of the minority carrier lifetime, mobility, and diffusion length are needed. Doping and the particulars of full device fabrication need to be worked out as well. Our growth scheme avoids using expensive single-crystal substrates and associated complex epitaxial structures, which have thus far hindered the market success of III-V solar cells. Metal foil substrates not only reduce cost at the material growth step, but also at downstream processing steps. For example, flexible foil substrates are a natural fit for roll-to-roll processing.^[36] They are robust, light-weight, and act as excellent barriers to the environment. Poly-InP grown using our technique shows great promise for high-efficiency, low-cost solar cells.

Acknowledgements

Many thanks to the contributors on this project: Zhibin Yu, Tae Joon Seok, Yu-Ze Chen, Rehan Kapadia, Kuniharu Takei, and Shaul Aloni, as well as our PIs Joel W. Ager, Ming Wu, Yu-Lun Chueh, and Ali Javey.

This work was supported by the Director, Office of Science, Office of Basic Energy Sciences, Materials Sciences and Engineering Division of the U.S. Department of Energy under Contract No. DE-AC02-05CH11231. A.J. acknowledges support from the World Class University program at Suncheon National University.

References

- [1] M.A. Green, K. Emery, Y. Hishikawa, W. Warta, *Prog. Photovoltaics Res. Appl.* 2011, *19*, 84-92.
- [2] C.J. Keavney, V.E. Haven, S.M. Vernon, in *Conf. Rec. 21st IEEE Photovoltaic Spec. Conf.* 1990, *1*, 141-144.
- [3] M.W. Wanlass, T.J. Coutts, J.S. Ward, K.A. Emery, in *Conf. Rec. 22nd IEEE Photovoltaic Spec. Conf.* 1991, *1*, 159-165.
- [4] J. Yoon, S. Jo, I.S. Chun, I. Jung, H.-S. Kim, M. Meitl, E. Menard, X. Li, J.J. Coleman, U. Paik and J.A. Rogers, *Nature* 2010, *465*, 329-333.
- [5] X.Y. Lee, A.K. Verma, C.Q. Wu, M. Goertemiller, E. Yablonovitch, J. Eldredge, D. Lillington, in *Conf. Rec. 25th IEEE Photovoltaic Spec. Conf.* **1996**, 53-55.
- [6] J.M. Zahler, K. Tanabe, C. Ladous, T. Pinnington, F.D. Newman, H.A. Atwater, *Appl. Phys. Lett.* **2007**, *91*, 012108.
- [7] J.M. Zahler, A. Fontcuberta i Morral, Chang-Geun Ahn, H.A. Atwater, M.W. Wanlass, C. Chu, P.A. Iles, in *Conf. Rec. 29th IEEE Photovoltaic Spec. Conf.*, **2002**, 1039- 1042.
- [8] K. Lee, K.-T. Shiu, J.D. Zimmerman, C.K. Renshaw, S.R. Forrest, *Appl. Phys. Lett.* **2010**, *97*, 101107.
- [9] T. Nakamura, T. Katoda, *J. Appl. Phys.* **1984**, *55*, 3064.
- [10] Y. Rosenwaks, Y. Shapira, D. Huppert, *Phys. Rev. B* **1991**, *44*, 13097-13100.
- [11] R.K. Ahrenkiel, D.J. Dunlavy, T. Hanak, *J. Appl. Phys.* **1988**, *64*, 1916.
- [12] R.K. Ahrenkiel, D.J. Dunlavy, T. Hanak, *Sol. Cells* **1988**, *24*, 339-352.
- [13] Y. Rosenwaks, Y. Shapira, D. Huppert, *Phys. Rev. B* **1992**, *45*, 9108-9119.
- [14] S. Bothra, S. Tyagi, S.K. Ghandhi, J.M. Borrego, *Solid-State Electron.* **1991**, *34*, 47-50.
- [15] D.D. Nolte, *Solid-State Electron.* **1990**, *33*, 295-298.
- [16] L. Jastrzebski, J. Lagowski, H.C. Gatos, *Appl. Phys. Lett.* **1975**, *27*, 537-539.
- [17] R. Venkatasubramanian, B.C. O'Quinn, J.S. Hills, P.R. Sharps, M.L. Timmons, J.A. Hutchby, H. Field, R. Ahrenkiel, B. Keyes, in *Conf. Rec. 25th IEEE Photovoltaic Spec. Conf.* **1996**, 31-36.
- [18] Y.C.M. Yeh, R.J. Stirn, *Appl. Phys. Lett.* **1978**, *33*, 401.
- [19] T. Saitoh, S. Matsubara, S. Minagawa, *Thin Solid Films* **1978**, *48*, 339-344.
- [20] T. Saitoh, S. Matsubara, S. Minagawa, *Jpn. J. Appl. Phys.* **1976**, *15*, 893-894.

- [21] T. Saitoh, S. Matsubara, S. Minagawa, *J. Electrochem. Soc.* **1976**, *123*, 403-406
- [22] T. Saitoh, S. Matsubara, *J. Electrochem. Soc.* **1977**, *124*, 1065-1069.
- [23] T. Saitoh, S. Matsubara, S. Minagawa, *Jpn. J. Appl. Phys.* **1977**, *16*, 807-812.
- [24] K.J. Bachmann, E. Buehler, J.L. Shay, S. Wagner, *Appl. Phys. Lett.* **1976**, *29*, 121.
- [25] R.L. Woo, R. Xiao, Y. Kobayashi, L. Gao, N. Goel, M.K. Hudait, T.E. Mallouk, R.F. Hicks, *Nano Lett.* **2008**, *8*, 4664-4669.
- [26] R.E. Algra, M.A. Verheijen, M.T. Borgstrom, L.-F. Feiner, G. Immink, W.J.P. van Enkevort, E. Vlieg, E.P.A.M. Bakkers, *Nature* **2008**, *456*, 369-372.
- [27] H. Gottschalk, G. Patzer, H. Alexander, *Phys. Status Solidi A* **1978**, *45*, 207-217.
- [28] P.I. Gaiduk, F.F. Komarov, V.S. Tishkov, W. Wesch, E. Wendler, *Phys. Rev. B* **2000**, *61*, 15785-15788.
- [29] ICDD PDF-2. Entry 00-032-0452. **2003**.
- [30] G.F. Alfrey, P.H. Borchers, *J. Phys. C: Solid State Phys.* **1972**, *5*, L275-L278.
- [31] A. Mooradian, G.B. Wright, *Solid State Commun.* **1966**, *4*, 431-434.
- [32] L. Artús, R. Cuscó, J.M. Martín, G. González-Díaz, *Phys. Rev. B* **1994**, *50*, 11552-11555.
- [33] W.J. Turner, W.E. Reese, G.D. Pettit, *Phys. Rev.* **1964**, *136*, A1467-A1470.
- [34] M. Bugajski, W. Lewandowski, *J. Appl. Phys.* **1985**, *57*, 521.
- [35] G. Perna, V. Capozzi, V. Augelli, T. Ligonzo, L. Schiavulli, G. Bruno, M. Losurdo, P. Capezzuto, J.L. Staehli, M. Pallara, *Semicond. Sci. Technol.* **2001**, *16*, 377-385.
- [36] M.H. Lee, N. Lim, D.J. Ruebusch, A. Jamshidi, R. Kapadia, R. Lee, T.J. Seok, K. Takei, K.Y. Cho, Z. Fan, H. Jang, M. Wu, G. Cho, A. Javey, *Nano Lett.* **2011**, *11*, 3425-3430.